Dynamic Smagorinsky model on anisotropic grids

By A. Scotti[1], C. Meneveau[1] AND M. Fatica[2]

Large Eddy Simulation (LES) of complex-geometry flows often involves highly anisotropic meshes. To examine the performance of the dynamic Smagorinsky model in a controlled fashion on such grids, simulations of forced isotropic turbulence are performed using highly anisotropic discretizations. The resulting model coefficients are compared with a theoretical prediction (Scotti *et al.*, 1993). Two extreme cases are considered: pancake-like grids, for which two directions are poorly resolved compared to the third, and pencil-like grids, where one direction is poorly resolved when compared to the other two. For pancake-like grids the dynamic model yields the results expected from the theory (increasing coefficient with increasing aspect ratio), whereas for pencil-like grids the dynamic model does not agree with the theoretical prediction (with detrimental effects only on smallest resolved scales). A possible explanation of the departure is attempted, and it is shown that the problem may be circumvented by using an isotropic test-filter at larger scales.

Overall, all models considered give good large-scale results, confirming the general robustness of the dynamic and eddy-viscosity models. But in all cases, the predictions were poor for scales smaller than that of the worst resolved direction.

1. Introduction

Since its introduction in the 1960's, a goal of LES has been to simulate complex turbulent flows. A complex flow is, by definition, characterized by regions were the physics of turbulence change, e.g., from homogeneous turbulence far from boundaries to near wall turbulence, etc. To capture the full gamut with a simple subgrid model without having to adjust constants in an *ad hoc* manner every time was a serious problem until recently. The introduction of the dynamic model (Germano *et al.*, 1991) to dynamically calculate the parameter(s) of the modeled sub-grid stress was a significant step towards making LES of complex flows possible without *ad hoc* adjustments. This model is able to self-adjust to the large scale flow in the correct fashion, for instance, shutting itself down near walls or in regions where the flow relaminarizes.

As a result, it has become possible to apply LES to study flows of increasing complexity (e.g. Akselvoll and Moin 1996 or see in this same volume Chan and Mittal, and Haworth and Jansen), which in turn requires the use of complex grids, either structured or unstructured. Complicated grid geometries in conjunction with

1 The Johns Hopkins University, Baltimore, MD 21218

2 Center for Turbulence Research

the dynamic model raise several questions. Consider, as an example, the flow past a 3-D bluff body: near the object, one needs to refine the grid in the spanwise directions. For a structured mesh, far downstream, the grid may be greatly expanded in the streamwise direction. Therefore, the grid can be strongly anisotropic, with the elements of the grid looking like sheets or pencils, depending on the kind of refinement imposed upstream. Hence, in the far-wake region one may have a situation where the turbulence is nearly isotropic, whereas the computational grid is highly anisotropic.

In LES, the grid filter is dictated by the computational mesh used to solve the equations (although, for methods other than spectral, it is difficult to give a precise definition of the filtering operator associated with a given discretization). Since classical eddy-viscosity models need as input a length-scale which is usually associated with the scale at which the filter operates, the problem arises in defining this length when, as a result of the anisotropy of the grid, the filter is defined by more than one length scale. For the Smagorinsky model, this problem was considered first by Deardoff (1970) and later by Schumann (1975), Lilly (1988) and Scotti *et al.* (1993), although the last two papers were only theoretical treatments.

On the other hand, other models such as the dynamic model do not in principle require a length scale to be specified. The question then arises whether the dynamic model is able to correctly simulate isotropic turbulence on anisotropic grids. The main goal of this work is to examine this question.

This issue is also of theoretical interest since, from the point of view of interaction among modes, local triadic interactions at small scales are fully available only to a limited amount of modes. Thus the small scales are exposed to a dynamic which is not the one typical of 3-D turbulence. It is natural then to expect that the SGS stress tensor should incorporate a correction originating only from the anisotropy of the grid.

The paper is organized as follows: in section 2 we briefly summarize the main result of Scotti *et al.* (1993) and set the notation that will be used throughout the paper; in Section 3 we discuss the simulations and how the results of different models will be compared. In showing the results, we have considered two categories of grids: pancake-like, when one direction is much better resolved than the other two, and pencil-like, when two directions are much better resolved than the third. Section 4 presents the results. Finally, in Section 5 a summary and discussion of the results is given.

2. Smagorinsky model on anisotropic grids

In this section, the results of Scotti *et al.* (1993) are briefly recalled. They are based on the assumption that the turbulence is isotropic and homogeneous, and that the largest and smallest scales at which the filter operates still lie within the inertial range. One begins by writing the Smagorinsky model as

$$\tau_{ij} = -2[L(\Delta_1, \Delta_2, \Delta_3)]^2 [2\tilde{S}_{lm}^2]^{1/2} \, \tilde{S}_{ij}. \tag{1}$$

Here Δ_1, Δ_2 and Δ_3 are the dimensions of the computational cell. For notational convenience and without lack of generality, let us assume $\Delta_1 \leq \Delta_2 \leq \Delta_3$. The

equivalent filter, via a collocation rule, is assumed to be a sharp cut-off filter in Fourier space, which corresponds to setting to zero all the modes outside the region $B = \{|k_1| < \pi/\Delta_1, |k_2| < \pi/\Delta_2, |k_3| < \pi/\Delta_3\}$, leaving the others unmodified.

By invoking an argument used first by Lilly (1967) an expression for $L(\Delta_1, \Delta_2, \Delta_3)$ was derived by requiring that

$$\varepsilon = - < \tau_{ij} \tilde{S}_{ij} >,$$

replacing τ_{ij} with the model and computing moments of the strain-rate tensor, assuming that the velocity field is characterized by a Kolmogorov isotropic spectrum on all resolved modes.

Introducing $\Delta_{eq} = (\Delta_1 \Delta_2 \Delta_3)^{1/3}$, $L(\Delta_1, \Delta_2, \Delta_3)$ can then be written as

$$L(\Delta_1, \Delta_2, \Delta_3) = C_s \Delta_{eq} f(a_1, a_2), \tag{2}$$

where $a_1 = \Delta_1/\Delta_3$ and $a_2 = \Delta_2/\Delta_3$ are the two aspect ratios of the grid, and $f \geq 1$ is a function equal to one if both ratios are equal to unity. C_s is the traditional Smagorinsky coefficient, which depends on the value of the Kolmogorov constant.

After evaluating the function f, a compact approximation for the result was given by Scotti *et al.* (1993)

$$f(a_1, a_2) \simeq \cosh \sqrt{4/27((\log a_1)^2 - \log a_1 \log a_2 + (\log a_2)^2)}. \tag{3}$$

Incidentally, we remark that the fact that $f \simeq 1$ for aspect ratios close to unity justifies the practice introduced by Deardoff (1970) of using Δ_{eq} as length scale, at least for aspect ratios close to unity. In the dynamic version of this model, with grid filtering denoted by tilde and test filtering by an overbar, the length-scale $L(\tilde{\Delta}_1, \tilde{\Delta}_2, \tilde{\Delta}_3)$ is computed according to

$$2[L(\tilde{\Delta}_1, \tilde{\Delta}_2, \tilde{\Delta}_3)]^2 = \frac{< L_{ij} M_{ij} >}{< M_{ij} M_{ij} >}, \tag{4}$$

where

$$L_{ij} = \overline{\tilde{u}_j \tilde{u}_i} - \overline{\tilde{u}}_i \overline{\tilde{u}}_j, \tag{4a}$$

and

$$M_{ij} = \left[\overline{[2\tilde{S}_{lm}^2]^{1/2} \tilde{S}_{ij}} - \left(\frac{\overline{\tilde{\Delta}}_{eq}}{\tilde{\Delta}_{eq}} \frac{f(\overline{a}_1, \overline{a}_2)}{f(\tilde{a}_1, \tilde{a}_2)} \right)^2 [2\overline{\tilde{S}}_{lm}^2]^{1/2} \overline{\tilde{S}}_{ij} \right], \tag{4b}$$

where we have made use of Eq. (2). If both test and grid filter have the same aspect ratios then Eq. (4) is closed; otherwise we can use Eq. (3) to compute f and check *a posteriori* its consistency.

3. Approach and validation

We run LES of isotropic turbulence in a box of side 2π with periodic boundary conditions. Turbulence is maintained by a forcing $\mathbf{f}$ that forces the largest modes ($k \leq 2$) with an intensity such that the energy injection rate $\mathbf{f} \cdot \mathbf{u}$ is fixed at a constant value $\varepsilon = 1.0$. The numerical scheme is the same as in Vincent and Meneguzzi (1991) and Briscolini and Santangelo (1994). It uses Adam-Bashforth 2 for time advancing, with $\Delta t = 0.001$. The nonlinear terms, written in rotational form, are evaluated pseudospectrally. Appendix A examines dealiasing for the AB2 scheme. The grids have mesh sides $(\Delta_1, \Delta_2, \Delta_3)$, with $\Delta_3 > \max\{\Delta_1, \Delta_2\}$, and aspect ratios $a_1 = \Delta_1/\Delta_3$, $a_2 = \Delta_2/\Delta_3$ ranging from 1 to 1/16. Grid filtering was performed with a sharp spectral cut-off setting to zero the modes outside the ellipsoid $B = \{\mathbf{k} \in R^3 \mid (k_1\Delta_1)^2 + (k_2\Delta_2)^2 + (k_3\Delta_3)^2 \leq 8/9\pi^2\}$, which has the advantage of partially removing aliasing errors (see appendix A). Test filtering was done at a scale twice as large in all directions.

For comparison, computations were performed using the classical non-dynamic Smagorinsky model with the Deardoff length scale and $C_s^2 = 0.026$, as well as with the Smagorinsky model corrected after Scotti *at al.* (1993) including $f(a_1, a_2)$ as evaluated from Eq. (3). In all cases the initial condition is assumed to be a random Gaussian field with $k^{-5/3}$ spectrum, random phase, and total kinetic energy equal to unity.

We wish to compare both large scale properties, such as total kinetic energy, derivative skewness in the worst resolved direction, and small scale properties, such as energy spectra near cut-off scale and the skewness in the best resolved direction (which is sensitive to the details of the small scales).

For isotropic turbulence we know that the spectral tensor in the inertial range is given by

$$Q_{ij}(\mathbf{k}) = <u_i(\mathbf{k})u_j(-\mathbf{k})> = (4\pi)^{-1}C_{\mathrm{K}}\varepsilon^{2/3}k^{-11/3}P_{ij}(\mathbf{k}), \tag{5}$$

where ε is the average dissipation, C_{K} is the Kolmogorov constant, and $P_{ij}(\mathbf{k})$ is the projector on the space orthogonal to $\mathbf{k}$. Also, we know that the skewness of the derivative is $O(-.5)$, although for LES the value attained is typically smaller due to the incomplete resolution of the small scales. We will compute the skewness in the $\alpha-$direction, defined as $S_\alpha = <(\partial\tilde{u}_\alpha/\partial x_\alpha)^3> / <(\partial\tilde{u}_\alpha/\partial x_\alpha)^2>^{3/2}$.

Due to the anisotropy of the grid, it is better to study 1-D premultiplied spectra, defined as

$$C(k_1) = \frac{\int_B 2\pi\varepsilon^{-2/3}k^{11/3}Q_{ii}(\mathbf{k})dk_2\,dk_3}{\int_B dk_2\,dk_3}.$$

For ideal Kolmogorov turbulence, where the spectral tensor is given by Eq. (5), $C(k_1)$ is a constant equal to the Kolmogorov constant $C_K \simeq 1.6$.

4. Results

To obtain a self-consistent estimate for the Smagorinsky constant C_s, we first run LES with the dynamic model with isotropic spherical test and grid filter on a 32^3 grid. After an initial transient the value stabilizes at $C_s^2 = 0.023 \pm 5\%$. Next, we

(a)
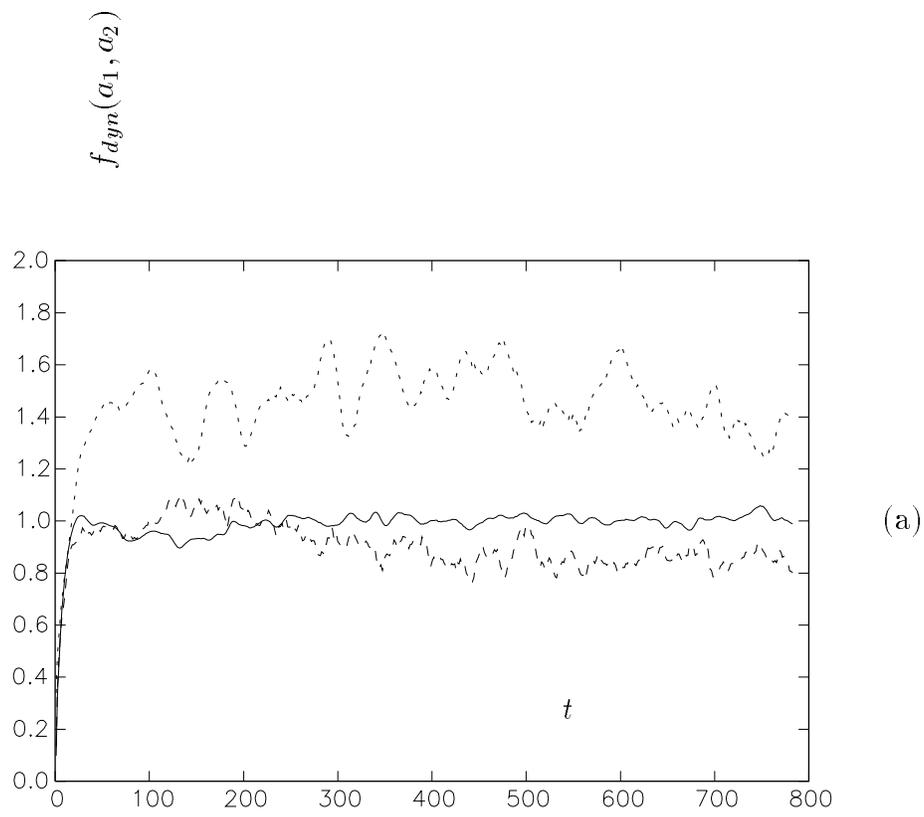
perform LES on anisotropic grids characterized by aspect ratios a_1 and a_2. The results are cast in terms of $f(a_1, a_2)$, by writing

$$f_{\mathrm{dyn}}(a_1, a_2) = \sqrt{\frac{< L_{ij} M_{ij} >}{2 < M_{ij} M_{ij} >}} \frac{0.023^{-1/2}}{\Delta_{eq}}.$$

Figure 1a shows the time evolution of $f_{\mathrm{dyn}}(a_1, a_2)$ for three cases: an isotropic grid on 32^3 modes, a pancake-like grid using a $256 \times 16 \times 16$ grid, and a pencil-like grid using $128 \times 128 \times 16$ modes.

In the same way we have computed the time averages of f_{dyn} for aspect ratios varying from $1/2$ to $1/16$. They are plotted in Figure 1b together with the value obtained from Eq. (3). We see that the dynamic model reproduces the correct trend for pancake-like grids, but fails with pencil-like grids. To examine the simulations more closely, we now focus on two extreme cases: a $256 \times 16 \times 16$ grid (pancake) and a $128 \times 128 \times 16$ grid (pencil). For each case, we compare the dynamic model with predictions of the non-dynamic Smagorinsky model and with the non-dynamic model but including the correction of Eq. (3).

4.1 Pancake-like

Figure 2 shows the total kinetic energy versus time for the three models considered. We see that the three models agree quite well. Also, the skewness in the least resolved direction does not show marked differences. We conclude that at the large-scale level, there is no impact on the model variations even at this high level of grid anisotropy. Next, we consider the behavior near the grid scale. The premultiplied 1-D spectrum is shown in Fig. 3. The traditional Smagorinsky-Deardoff case shows a strong peak at wavenumber $k_1 \sim 10$. The modified Smagorinsky case remains constant at small wavenumbers and dies out at high wavenumbers without showing any pile-up. The dynamic model falls somewhere in between, but the value is higher than the expected value of C_K. All models show a rapid decay at wavenumbers above 10.

The fact that all three models decay for $k_1 > 10$ means that those modes that cannot have access to all the local triadic interactions experience a high drain of energy so that they do not display a Kolmogorov scaling. It appears unlikely that any modification of a scalar eddy-viscosity model could compensate for this behavior.

The analysis of the derivative skewness in the well-resolved direction shows no real difference.

4.2 Pencil-like

As already mentioned, the dynamic model gives a value for f_{dyn} which is smaller than one, in contrast with the theoretical expression, which implies that f must be bigger than one. If we look at the large-scale parameters of the flow, energy and skewness in the least resolved direction (Fig. 4) we see that the three models again give similar answers; note the small value of the skewness in the worst resolved direction. But if we consider parameters that are more sensitive to the small scale

$E(t)$

(a)
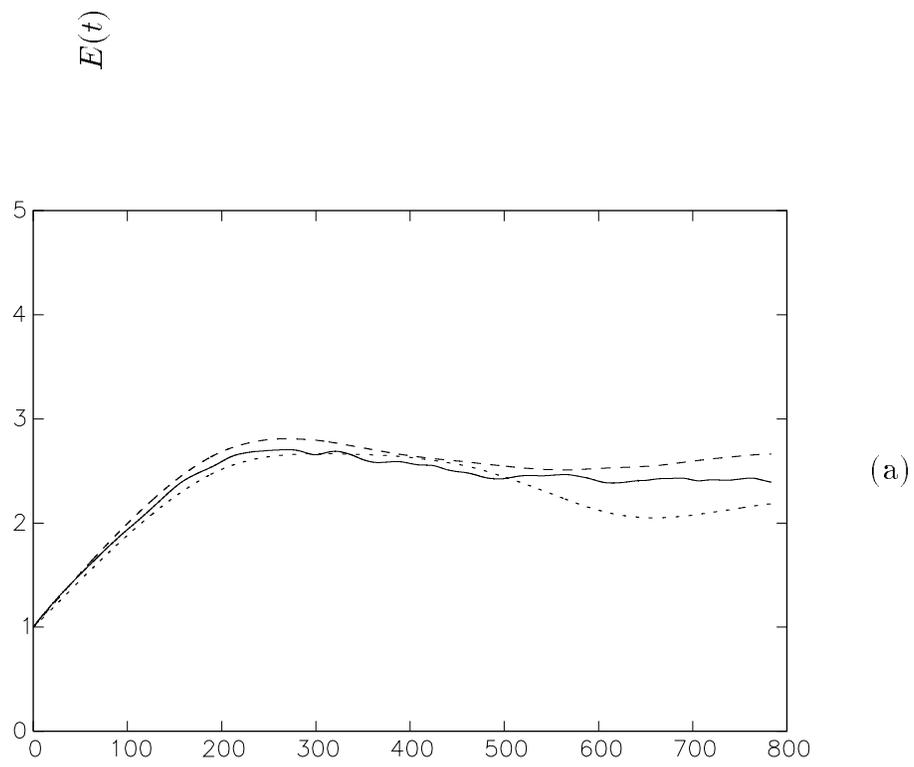
$S_3(t)$

behavior, we notice marked differences. For the dynamic model the Kolmogorov constant is too large, about twice as much as expected (Fig. 5). Therefore, the "underestimation" of f brings consequences that cannot be ignored at the scales near the least resolved direction. Again, scales between the least and best resolved directions are much less energetic than the Kolmogorov spectrum, as is clear from the rapid drop of the premultiplied spectrum above $k_1 = 16$. On the other hand, the modified Smagorinsky model gives too small a value, probably due to overdamped modes near $k \sim \frac{\pi}{\Delta_3}$. Finally, the skewness in the best resolved direction is consistent with these differences: the smaller the skewness is in magnitude, the more the energy piles up.

4.3 Discussion

The strongest discrepancy between the theoretically and dynamically determined $f(a_1, a_2)$ was observed for the case of highly pencil-like grids. For this case, the premultiplied spectrum of the dynamic model case showed considerable pile-up, as evidenced by much higher values of $C(k_1)$. In order to understand the causes of this behavior, we recall that the dynamic model computes L by sampling the turbulence between grid and test filter. It could be argued that for pencil-like grids these modes behave essentially as 2D turbulence, with the vorticity aligned in the x_3 direction and a concomitant change in the dynamics. To focus on the relevant scales, we have analyzed the vorticity band-pass filtered between test and grid filter (i.e. the statistics of $\omega' = \tilde{\omega} - \overline{\omega}$). We find that the variances are not isotropic, and that $\omega_1'^2/\omega_3'^2 \sim \omega_2'^2/\omega_3'^2 \sim 0.75$, i.e. the flow is not quite 3-D but not 2-D either. More directly related to the small value of L or f_{dyn} obtained from the dynamic model, in Fig. 6 we show the PDF of $L_{ij}M_{ij}$ (solid line). The curve is almost symmetrically distributed around the origin, and the average value, while positive, is very small ($< L_{ij}M_{ij} >= 4.80$). $L_{ij}M_{ij}$ can be regarded as a measure of energy transfer from large to small scales, with negative values meaning energy backscatter. If we now compute the same PDF but using an isotropic test filter at a scale $2\Delta_3$ in all three directions, we see that the shape of the PDF changes, being now skewed to the right (symbols in Fig. 6). The mean value is now $< L_{ij}M_{ij} >= 31.66$. Therefore, by sampling larger scales that are more isotropic, the dynamics of the energy transfer changes noticeably.

This observation suggests that in order to improve the performance of the dynamic model in such extreme cases of grid anisotropy, it may be advisable to use a test filter which is isotropic, with a length scale twice as large as the worst resolved scale. In this case, the grid and test anisotropies differ, and this must be taken into account explicitly in the dynamic model formulation. We now implement the dynamic model with Eq. (4b) for M_{ij}, using the expression given in Eq. (3) for $f(\overline{a}_1, \overline{a}_2)$ and $f(\tilde{a}_1, \tilde{a}_2)$. Using this formulation on a $128 \times 128 \times 16$ simulation yields the result shown in Fig. 6. The time trace of f (Fig. 6) shows that it oscillates around an average value of $1.44 \pm .067$, much closer to the expected value of 1.34 than the value of 0.8 obtained with pencil-like test filtering. At large scales the difference between this run and the previous one is small. On the other end, at small scales the situation changes as now the premultiplied spectrum (Fig. 7) lies

$C(k_1)$

(a)

k_1
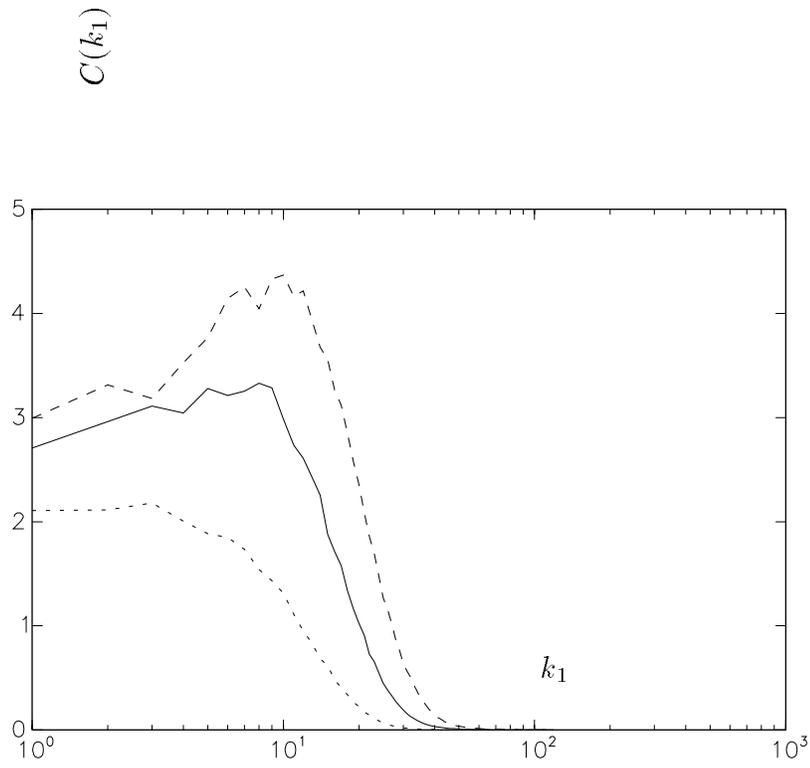
$S_1(t)$

flat at 1.4 for $k_1 < 10$, very close to the expected value for C_K. The skewness in the best resolved direction agrees well with the one calculated from the modified Smagorinsky model.

5. Conclusions

We have run several LES of forced isotropic turbulence on anisotropic grids, using three different Smagorinsky models. All three models are able to satisfactorily reproduce the very large scales of the flow. This result confirms the general robustness of the dynamic model even for the extreme cases considered in this work (see Jiménez (1995) for further observations on the dynamic model's robustness). However, none of the models considered is able to give a correct representation of the scales smaller than the worst resolved direction, where spectra are strongly damped below Kolmogorov values. This is probably due to the fact that the transfer of energy at very small scales is affected by the lack of similar modes in one or more directions. For a related study on the effect of grid anisotropy on velocity components and stress anisotropy, see Kaltenbach (1996).

For the model performance at scales near the cut-off in the worst resolved direction, we need to distinguish between pancake grids and pencil grids. For pancake-like grids, the non-dynamical Smagorinsky model modified after Scotti *et al.* (1993) and the dynamic model give reasonably good results, while the conventional Smagorinsky model using the Deardoff prescription for Δ_{eq} shows excessive pile up of energy at scales close to the largest mesh size. The anisotropy factor computed from the dynamic model shows an increasing trend with anisotropy in accord with the theoretical prediction, although the numerical value is somewhat smaller. For pencil-like grids, the Smagorinsky-Deardoff model as well as the modified version give good results, with the modified version yielding slightly better results. On the other hand, the dynamic model exhibits insufficient dissipation of energy, as shown by the fact that the anisotropy factor f_{dyn} becomes smaller than one, and reflected in that small scales have excessive energy as compared to the Kolmogorov value.

It would appear that in this particular case the strength of the dynamic model becomes its weak point. The dynamic model computes the unknown factor from information derived from the smallest resolved scales. But in the case of highly anisotropic grids, these scales experience a dynamic which is different from the usual one due to the missing modes at large wavenumbers. This in turn affects the resolved non-linear interactions embodied in the term $L_{ij}M_{ij}$, which is what the dynamic model samples. Specifically, the number of events during which energy is transferred forward is decreased, which could actually be explained by a partial 2-dimensionalization of the flow at these scales.

A proposed improvement is to move the test filter towards larger scales, where the combination of more energetic modes and more realistic triadic coupling allows a more faithful representation of how energy is exchanged. Indeed, simulations done with an isotropic test filter at twice the worst resolved scale show improved results. Perhaps not surprisingly, this conclusion is similar to one reached by others in the context of dynamic LES using non-spectral numerical methods, such as low-order

$E(t)$

(a)

$S_3(t)$
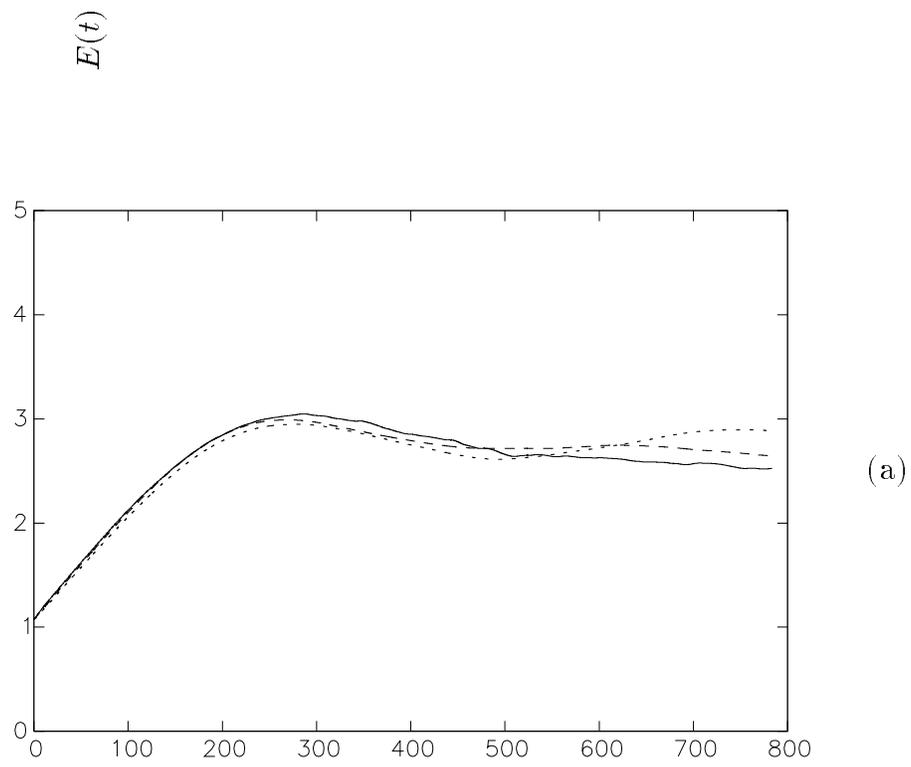
finite differences. There, it has been found advisable to "prefilter" the results and shift the test filter to larger scales (Ferziger 1996, Lund 1996) so that the dynamic model is not strongly affected by numerical errors occurring near the grid scale.

Acknowledgments

REFERENCES

AKSELVOLL, K. & MOIN, P. 1996 Large-eddy simulation of turbulent confined coannular jets. *J. Fluid Mech.* **315,** 387.

BRISCOLINI, M. & SANTANGELO, P. 1994 The non-Gaussian statistics of the velocity field in low-resolution large-eddy simulations of homogeneous turbulence. *J. Fluid Mech.* **270,** 199.

CANUTO, C., HUSSAINI, M.Y., QUARTERONI, A., ZANG, T.A. 1988 *Spectral methods in fluid dynamics. Springer-Verlag.*

DEARDOFF, J. W. 1970 A numerical study of three-dimensional turbulent channel flow at large Reynolds numbers. *J. Fluid Mech.* **41,** 453.

FERZIGER J. 1996 Personal communication.

GERMANO, M., PIOMELLI, U., MOIN, P. & CABOT, W. H. 1991 A dynamic subgrid-scale eddy viscosity model. *Phys. Fluid A.* **48,** 273-337.

JIMÉNEZ, J. 1995 On why dynamic subgrid-scale models work. *Annual Research Briefs.* Center for Turbulence Research, NASA Ames/Stanford Univ., 25-34.

KALTENBACH, H-J 1996 Cell aspect ratio dependence of anisotropy measures for resolved and subgrid scale stresses. Preprint.

LILLY, D. K. 1967 The representation of small-scale turbulence in numerical simulation experiments. *Proceedings of the IBM Scientific Computing Symposium on Environmental Science.* **320-1951,** 195.

LILLY, D. K. 1988 The length scale for sub-grid-scale parameterizaion with anisotropic resolution. *Annual Research Briefs.* Center for Turbulence Research, NASA Ames/Stanford Univ., 3-9.

LUND, T. 1996 Personal communication.

ROGALLO, R. S. 1977 An ILLIAC Program for the Numerical Simulation of Homogeneous Incompressible Turbulence. *NASA TM-81315.*

SCHUMANN, U. 1975 Subgrid scale model for finite difference simulations of turbulent flows in plane channels and annuli. *J. Comp. Phys.* **18,** 386.

SCOTTI, A., MENEVEAU, C. & LILLY, D. K. 1993 Generalized Smagorinsky model for anisotropic grids. *Phys. Fluid A.* **5,** 2306-2308.

VINCENT A. & MENEGUZZI M. 1991 The spatial structure and statistical properties of homogeneous turbulence. *J. Fluid Mech.* **225,** 1.

$C(k_x)$

$S-1(t)$

(a)

k_x
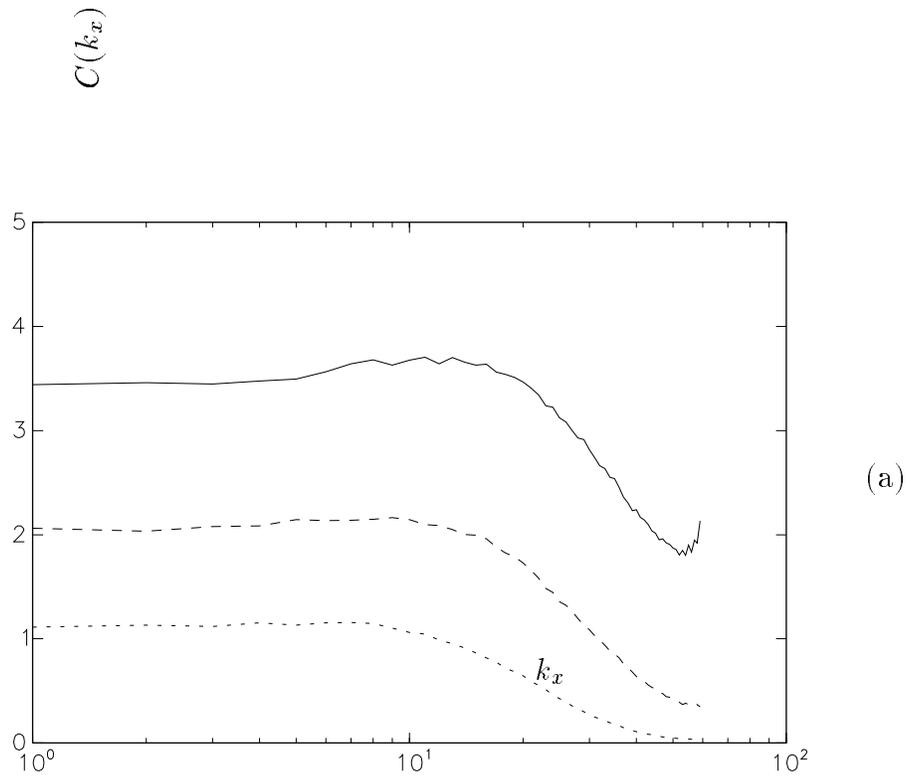
Appendix A

We assume that the computational domain is covered by $N_1 \times N_2 \times N_3$ points and $\mathbf{i}, \mathbf{j}$ and $\mathbf{l}$ are unit vectors in the x, y, and z directions. It is well known (see Canuto et al. (1987)) that the pseudospectral treatment of a 3-D convolution product $\sum_{\mathbf{m}+\mathbf{n}=\mathbf{k}} a(\mathbf{m})b(\mathbf{n})$ introduces an error. If we denote with $w_{\mathbf{k}}$ the true convolution product and with $W_{\mathbf{k}}$ the calculated one, the following relation holds:

$$W_{\mathbf{k}} = w_{\mathbf{k}} + \sum_{j=1}^{7} \mathcal{W}_j$$

where the seven extra terms have the form

$$\mathcal{W}_j = \sum_{\mathbf{m}+\mathbf{n}=\mathbf{k}+\mathbf{e}_j} a(\mathbf{m})b(\mathbf{n})$$

and

$$\mathbf{e}_1 = \pm N_1 \mathbf{i}, \ \ \mathbf{e}_2 = \pm N_2 \mathbf{j}, \ \ \mathbf{e}_3 = \pm N_3 \mathbf{l},$$

$$\mathbf{e}_4 = \pm N_1 \mathbf{i} \pm N_2 \mathbf{j}, \ \ \mathbf{e}_5 = \pm N_1 \mathbf{i} \pm N_3 \mathbf{l}, \ \ \mathbf{e}_6 = \pm N_3 \mathbf{l} \pm N_2 \mathbf{j},$$

$$\mathbf{e}_7 = \pm N_1 \mathbf{i} \pm N_2 \mathbf{j} \pm N_3 \mathbf{l}.$$

The last four terms, (double and triple aliased) can be set to zero if we adopt an elliptical truncation, i.e. , if we set to zero all the modes such that

$$\left(\frac{k_1}{N_1}\right) + \left(\frac{k_2}{N_2}\right) + \left(\frac{k_3}{N_3}\right) \geq \frac{2}{9}.$$

The proof is by inspection.

To remove the single aliased terms we can resort to phase shift. If we premultiply all the modes by a factor $e^{i\mathbf{k}\cdot\theta}$, $\theta \in [0, 2\pi] \times [0, 2\pi] \times [0, 2\pi]$, compute the convolution sum and multiply the result by $e^{-i\mathbf{k}\cdot\theta}$, the aliased terms now are $e^{\pm i\theta_j N_j} \mathcal{W}_j$, $j = 1, 2, 3$, i.e. we have shifted their phase by an amount $\pm\theta_j N_j$. If we do the same thing one more time, but this time $\theta \rightarrow \theta + (\pi/N_1, \pi/N_2, \pi/N_3)$ and take the average of the results, the aliased terms, being out of phase, will cancel exactly. However, this requires doubling the number of FFT's required for each term to be dealiased. Rogallo (1977) showed that for a multistep scheme such as even-order Runge-Kutta, it is possible to control the growth of aliasing essentially at no extra cost. Indeed, let us consider the typical step of a 2nd order Runge-Kutta:

$$u^{n+1} = u^n + \frac{\Delta t}{2}(F_1 + F_2)$$

with F_i's being the non-linear terms evaluated recursively. It is important to notice that to 0th order in Δt they are identical. Therefore, if F_1 is evaluated with a shift θ and F_2 with shift $\theta + (\pi/N_1, \pi/N_2, \pi/N_3)$, their sum to 0th order is dealiased, leaving possibly a contribution to first order. Therefore, the global effect of aliasing is

$P(L_{ij}M_{ij})$

$(L_{ij}M_{ij})$

(a)

f_{dyn}
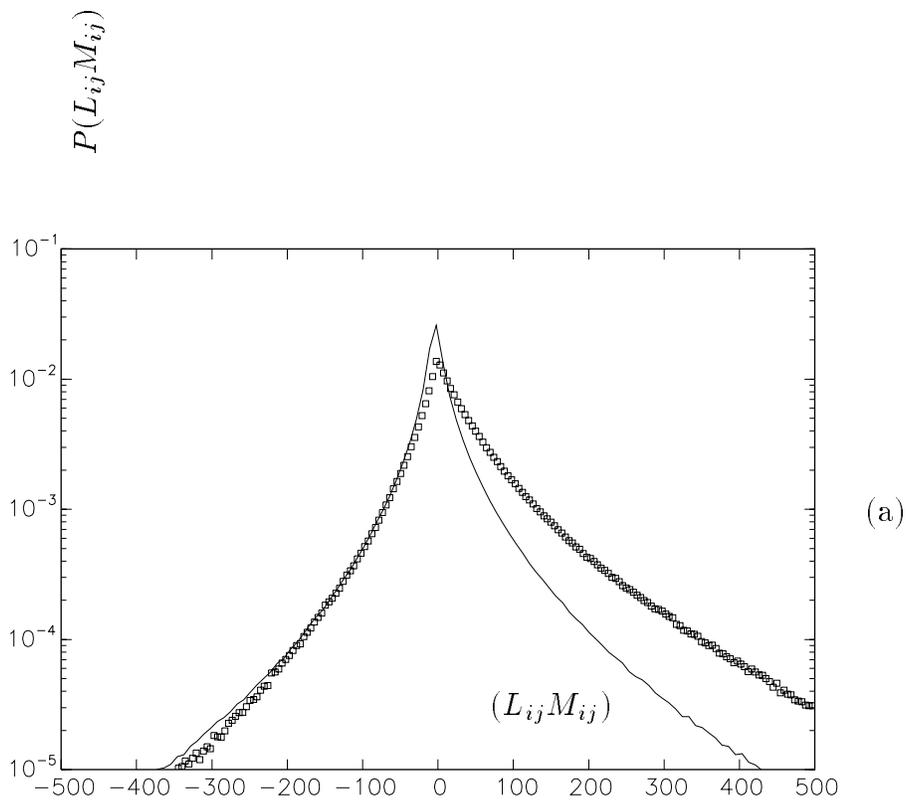
pushed to second order. Choosing θ randomly at each time step further ensures that the error does not accumulate over time. Nevertheless the RK-2 method requires doubling the FFT's for each time step.

In our computation we have used an AB2 scheme, which schematically can be written as

$$u^{n+1} = u^n + \frac{\Delta t}{2}(3F^n - F^{n-1})$$

with obvious meaning of the symbols. Although to 0th order the alias terms are identical in F^n and F^{n-1}, it is clear that there is no way in which a combination of phase shifts can cancel them exactly, since the equation
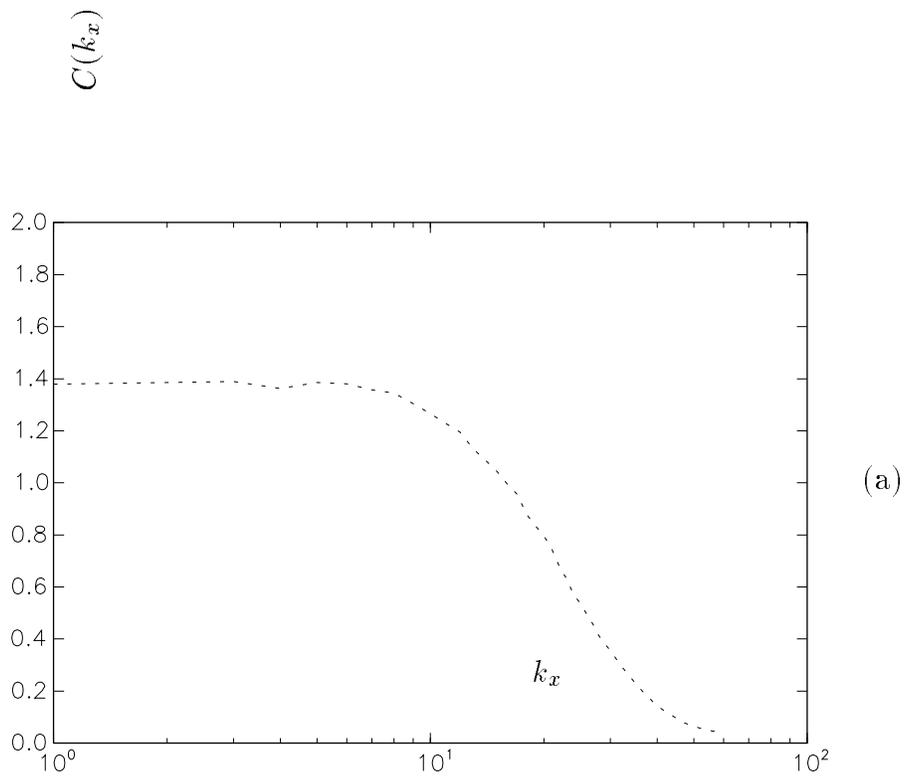
$$3e^{i\alpha N} - e^{i\beta N} = 0$$

does not have solutions for $\alpha, \beta \in [0, 2\pi]$.

However, by successive phase-shifts it is still possible to ensure that the error does not accumulate. If n is even, the shift is chosen randomly; if n is odd, the shift is chosen to be the shift of the previous time step plus $(\pi/N_1, \pi/N_2, \pi/N_3)$. After m time steps, the solution can be written as

$$u^{n+m} = u^n + \frac{\Delta t}{2}[3(F^n + F^{n+1} + F^{n+2} + \cdots + F^{n+m})$$
$$- (F^{n-1} + F^n + F^{n+1} + \cdots + F^{n+m-1})].$$

In the two bracketed sums, to the lowest order, all but a few aliased terms (typically the first and/or the last) cancel out. This proves that the error does not accumulate, and that after m steps the aliasing is still $O(\Delta t)$, no matter how big m is. Again, the randomness prevents accumulation at higher orders. We have compared results obtained with this dealiasing technique with results obtained by zero padding (2-rule in the worst resolved direction) without finding any noticeable difference.

$C(k_x)$

$S_1(t)$

(a)

k_x